Directed yeast genome evolution by controlled introduction of trans-chromosomic structural variations

Bin Jia[1,2,*] , Jin Jin[1, 2,*] , Ming-Zhe Han[1, 2], Bing-Zhi Li[1, 2] & Ying-Jin Yuan[1,2,†]

[1] Frontier Science Center for Synthetic Biology and Key Laboratory of Systems Bioengineering (Ministry of Education), School of Chemical Engineering and Technology, Tianjin University, 300072 Tianjin, China.

[2] Collaborative Innovation Center of Chemical Science and Engineering (Tianjin), Tianjin University, 300072 Tianjin, China.

[*] Authors contributed equally to this work.

[†] Corresponding author (email: yjyuan@tju.edu.cn)

Abstract

Background: Naturally occurring structural variations (SVs) are a considerable source of genomic variation and can reshape chromosomes 3D architecture. The synthetic chromosome rearrangement and modification by loxP-mediated evolution (SCRaMbLE) system has been proved to generate random SVs to impact phenotypes and thus constitutes powerful drivers of directed genome evolution. However, controllable methods to introduce complex SVs and revealing the related molecular mechanism has so far remained challenging.

Results: We develop a SV-prone yeast strain by using SCRaMbLE with two synthetic chromosomes, synV and synX. An heterologous biosynthesis pathway allowing a high throughput screen for increased yield of astaxanthin is used as readout and a proof of

concept for the application of SV in industry. We report here that complex SVs, including a pericentric inversion and a trans-chromosomes translocation between synV and synX, result in two neochromosomes and a 2.7-fold yield of astaxanthin. We mapped genetic targets contributing to higher astaxanthin yield and demonstrated the SVs can led to large reorganization of the genetic information along the chromosomes. We also used the model learned from the aforementioned random screen and successfully harnessed the precise introduction of trans-chromosomes translocation and pericentric inversions by rational design.

Conclusions: Our work provides an effective tool to not only accelerate the directed genome evolution but also reveal mechanistic insight of complex SVs for altering phenotypes.

Key words: Directed genome evolution, Structural variations, SCRaMbLE, Synthetic genome, Synthetic biology

Introduction

Chromosomes are highly dynamic objects that often undergo large structural variations(SVs), which in turn can reshape chromosomes and impact phenotypes[1-11]. Naturally occurring SVs comprised both unbalanced SVs that are copy number variations including deletions and duplications, and balanced SVs that are copy number neutral including inversions and translocations[12]. Both the unbalanced SVs and balanced SVs can modify the 3D architecture of the chromosomes and potentially affect genetic functioning, which contributed to the genome evolution. For example,

Selmecki.et al showed tetraploids yeast undergo significantly faster adaptation in a poor carbon source environment with larger deletion of chromosomes. [13]. Li.et al found that deletion of left arm of synthetic chromosome X and duplication of chromosome VIII (trisomy) lead to increased rapamycin resistance in yeast[14]. With the development of genome medicine, it is indicated reciprocal translocation between chromosomes have contributed to several human diseases, for instance, chronic myeloid leukemia (chromosomes 9 with 22) and Mobius-like syndrome (chromosomes 1 with 2)[15] [16]. In addition, pericentric inversion of chromosome 9 is one of the most common chromosomal abnormalities and can be associated with ambiguous genitalia in children[17]. It is challenge to map the balanced SVs than unbalanced SVs due to the copy number neutral. So far, the detailed molecular mechanism underlying balanced SVs remained unexplored due to lack of cell models.

The baker yeast (Saccharomyces cere*visiae*) appreciated for the availability of its powerful genetic tools, biosafety and fast growth rate has been used extensively in synthetic biology for industrial purposes. High-throughput phenotypic screenings have been employed to identify genome-wide deletions and duplications that increase the yield of yeast synthetic biology products. The completion of the yeast gene-knockout collection (YKOC) has enabled the analysis of synthetic genetic interactions[18]. The construction of segmental duplications covering the whole *S. cerevisiae* genome has been used to produce strains with enhanced tolerance to stresses[19]. Many rational design strategies, including overexpression and downregulation, are time-consuming because identifying gene targets remains an challenge due to the complexity of genetic

networks [20][Rapid prototyping of microbial cell factories via genome-scale engineering. Biotechnol Adv 2015, 33:1420-1432.]. Many successful examples demonstrate that the synthetic yeast chromosome could be reprogrammed for various purposes with greatly enhanced metabolic capacity[21-23]. The Synthetic Chromosome Rearrangement and Modification by LoxP-mediated Evolution (SCRaMbLE) technology have been developed to generate larger-scale SVs[14, 21-29]. SCRaMbLE is a powerful approach to study how chromosomal architecture impacts phenotypes and can be to mimic the Darwinian evolution process in the test tube for targeted phenotypes. Thus, SCRaMbLE can be viewed as natural molecular tools for directed genome evolution by iterative rounds of mutagenesis and screening or selection on the genome scale. So far, SCaMbLE has been used for directed genome evolution mainly with signal synthetic chromosome.

In this work we report that one by using SCaMbLE and two synthetic chromosomes, can for the first time creates chromosome inversion and translocation events on a larger scale and at a higher frequency. Introducing the same yeast cell with two synthetic chromosomes, each containing hundreds of non-directional loxPsym sites positioned downstream of non-essential genes and major landmarks provides a novel approach to genome reorganization especially SVs. We evaluate the effects of SVs on the enhanced production of an exogenous but commercially valuable terpenoid, astaxanthin. Two cycles of SCRaMbLE were used to iteratively generate complex SVs and improve the astaxanthin yield. We used the high-resolution chromosome conformational capture (Hi-C) sequencing approach to investigate the 3D conformations of chromosomes with

complex SVs[30], and observed an inversion spanning the centromere and a translocation between synV and synX. We developed a method to precisely reconstitute the translocations and inversions, and recaptured their combined effects on increasing the yield of astaxanthin by 2.7-fold. Our work thus provides a new toolkit for directed evolution of genomic assembly and reorganization.

Results

SCRaMbLE with two synthetic chromosomes for directed genome evolution

To investigate more complex SVs and biosynthesis pathways, we used the haploid strain SYN510 containing both synV with 176 loxPsym sites[31] and synX with 245 loxPsym sites[32] for the biosynthesis of astaxanthin. Astaxanthin is the end metabolite of the MVA pathway; it has tremendous antioxidant activity and is widely used in nutraceuticals, cosmetics and aquaculture[33, 34]. The astaxanthin biosynthesis pathway consists of 5 genes. *CrtE*, *CrtI* and *CrtYB* are involved in carotenoid biosynthesis, after which a reticular metabolic pathway with β-carotene ketolase (CrtW) and β-carotene hydroxylase (CrtZ) performs a two-step hydroxylation and ketolation reaction(Supplementary information, Fig. 1a). Our previous study demonstrated that the combination of Aa_CrtZ–BDC263_CrtW showed lower intermediate accumulation and achieved better astaxanthin yield[35]. To increase the stability of the astaxanthin biosynthesis pathway, all five genes were assembled together and integrated at the *YEL063C*/*CAN1* locus of synV to generate the yeast strain YJJ001 (Fig. 1a). It has been reported that the pCRE4 plasmid (pGal1-Cre-EBD-tCYC1) has tight control of Cre

111 recombinase and can be used for Multiplex SCRaMbLE Iterative Cycling (MuSIC).
112 Thus, the pCRE4 plasmid with a Ura3 marker was transformed into YJJ001 for the
113 control of SCRaMbLE.
114
115 In the first cycle of SCRaMbLE, strain YJJ168 was selected from the SCRaMbLEd
116 yeast pool due to its dark red pigmentation (Supplementary information, Fig. 1b). To
117 generate more complicated SVs and the desired phenotype, we used YJJ168 for the
118 second cycle of SCRaMbLE to yield another SCRaMbLEd strain, YJJ432. To identify
119 the chromosome SVs in haploids caused by SCRaMbLE, we deep sequenced YJJ168
120 and YJJ432. As shown in Fig. 1a and Supplementary information, Fig. 2, a 3 kb deletion
121 (YJL218W-YJL217W), a 1 kb inversion (YER044C) and a 210 kb pericentric inversion
122 (YJL052C-A-YJR071C) with 127 genes were observed in the SCRaMbLEd strain
123 YJJ168. It is interesting that the upstream and downstream of inversions of YJL052C-
124 A-YJR071C were on the left arm and right arm of synX, respectively. In other words,
125 this inversion spanned the centromere of synX. As an iterated SCRaMbLEd strain from
126 YJJ168, YJJ432 was observed to contain not only all the same SVs as YJJ168 but also
127 a inversion of YJL170C-YJL158C and a trans-chromosomictranslocation. It is noted
128 that the trans-chromosomictranslocation caused an exchange of 59 kb from the right
129 arm of synV and 74 kb from the right arm of synX that had not previously been reported.
130 From the sequencing data above, we find that the second-generation strains can inherit
131 genotypic SVs from first-cycle SCRaMbLEd strains. PCR verification of novel
132 junctions also confirmed that inversion and translocation events occurred in YJJ168 and

133 YJJ432 (Supplementary information, Fig. 3).

134

135 To investigate the structural organization of the chromosome SVs, Hi-C contact maps
136 (Fig. 1b) and 3D representations (Fig. 1c) of synV and synX were generated from
137 YJJ001, YJJ168 and YJJ432. The contact maps of synV and synX in YJJ168 and
138 YJJ432 showed several new interactions, indicating large-scale rearrangements in both
139 SCRaMbLEd strains. YJJ168 exhibited a new interaction indicating a large inversion
140 (YJL052C-A-YJR071C) event. The contact map of YJJ432 revealed three new
141 interactions caused by the large inversion (YJL052C-A-YJR071C), one inversion
142 (YJL170C-YJL158C) in synX and one translocation between the right arm of synV
143 (YJR130C) and the right arm of synX (YER164W). A three-dimensional model of the
144 16 yeast chromosomes and amplified chromosomes of synV and synX are provided in
145 Fig. 1c. The centromeres gather at the spindle pole, and all chromosomes are clustered
146 by the centromeres at one pole of the nucleus. The telomeres are clustered at the other
147 end. The 3D representations show that the average trajectories of chromosomes in
148 YJJ168 and YJJ432 did not appear to be substantively altered compared with those in
149 YJJ001, with the synthetic chromosomes neighboring the same chromosomes as the
150 native ones. New connections were generated in synX of strain YJJ168 and strain
151 YJJ432 due to the inversion spanning the centromere. In strain YJJ432, the right arms
152 of synV and synX generate two new connections because of the translocation between
153 synV and synX (the area within the dashed oval). It is indicated that the translocation
154 on the right arm of synV has a closer spatial distance with synX and consequently has

155 stronger interactions.

156

157 Meanwhile, the two SCRaMbLEd strains and YJJ001 were subjected to fermentation
158 experiments in YPD medium, and the astaxanthin yield was analyzed by high-
159 performance liquid chromatography (HPLC). As illustrated in Fig. 1d, the astaxanthin
160 yield in strain YJJ001 was 0.61 mg/g DCW, and the astaxanthin yield of the two
161 SCRaMbLEd strains (YJJ168 and YJJ432) was increased, to 0.90 and 2.7 mg/g DCW,
162 respectively. The astaxanthin yield was increased 1.48- to 4.43-fold in the SCRaMbLEd
163 strains compared with the nonSCRaMbLEd parent strain. These results revealed the
164 new interactions of synthetic chromosomes in SCRaMbLEd strains via Hi-C
165 technology. SCRaMbLE strains provide sufficiently detectable SVs, indicating that the
166 SCRaMbLE system provides a driving force to alter cell phenotypes through
167 rearranging gene order and number.

168

169 **Reorganization of the genetic information on the regions of SVs**

170 The pericentric inversion and trans-chromosomic translocation alter the spatial
171 positions of the breakpoint-flanking regions, which may which may led to large
172 reorganization of the genetic information along the chromosomes. To explore whether
173 the genetic information in the breakpoint-flanking regions were affected, we examined
174 transcription profile on the 20 kb regions upstream and downstream of the two loxPsym
175 breakpoints. As shown in Fig. 2a, the upstream and downstream regions of the
176 breakpoints of the pericentric inversion in YJJ168 were named A, B, C, and D,

177 respectively. We first observed changes in the transcription levels of YJL053W,
178 YJL052C-A and YJL052W near the left breakpoint and the transcription levels of
179 YJL067C, YJL070C and YJL071W near the right breakpoint. In the whole 80 kb region
180 consisting of A, B, C and D, 19 of 51 genes showed changes in expression
181 (Log2FoldChange > 1-fold) compared with the control strain YJJ001, with 1 and 18
182 gene downregulated and upregulated, respectively. Around the left breakpoint, the
183 changes in YJL052C-A and YJL052W were the most obvious, whereas around the right
184 arm recombination site, the change in YJR070C was the most obvious. Similarly, the
185 regions upstream and downstream of the breakpoint in the right arm of synV and the
186 breakpoint in the right arm of synX in YJJ432 were labeled E, F, G, and H, respectively
187 (Fig. 2b). Compared with the control strain, 15 of the 38 genes in these regions
188 exhibited changed expression (Log2FoldChange > 1-fold), with 2 and 13 genes
189 downregulated and upregulated, respectively. The results indicated that the expression
190 of genes in the breakpoint-flanking regions was indeed affected by different types of
191 SVs. To further quantify the interactions of the recombination sites, we counted the
192 interaction values of the four points on the interaction matrix of YJJ168 and YJJ432
193 and counted the differences between different interaction domains (areas marked by
194 boxes in Supplementary information, Fig. 4). As the results show, regions A and C and
195 regions B and D had significant interactions in inversion strains YJJ168 and YJJ432. In
196 translocation strain YJJ432, the interactions of regions E and H and F and G were
197 increased as a result of the greater proximity of the right arm of synV (YJR130C) to
198 synX and the right arm of synX (YER164W) to synV. These results further indicate that

199 two sites that are closer in space have greater interaction. It is spectacular that the
200 pericentric inversions and trans-chromosomes translocation changed larger number of
201 genes position and the transcription direction, which affected the transcription levels of
202 genes in the regions nearby the breakpoint of SVs[36].

203 **Mapping of genetic targets contributing to higher astaxanthin yield**

204 To identify the genetic targets with regard to the improvement of astaxanthin yield, the
205 above down-regulated genes and up-regulated genes in the regions nearby the
206 breakpoint of SVs were knocked out and overexpressed in the strain YJJ001 for
207 fermentation assay, respectively. As illustrated in Fig. 3a, compared to the control strain,
208 astaxanthin yields were significantly increased in strains with YJR086W, YJR123W
209 and YJR135C over-expression strain. The function of these three genes are briefly
210 described in Table 2. Although the exact reason for these genes to be beneficial to
211 astaxanthin yield remains to be elucidated, it is possible to speculate the mechanism
212 resulting in the favorable changes of this phenotype from functions previously
213 described in the literature. The result indicated upregulated these genes have
214 contributed to higher astaxanthin yield.

215 To further explore the global affection of chromosomal rearrangements on metabolic
216 pathways, enrichment analysis of transcriptomics was used to identify differentially
217 transcribed genes with known functions involved in KEGG pathways. Several genes
218 involved in terpenoid backbone biosynthesis, ergosterol biosynthesis and citrate cycle
219 were upregulated in the YJJ168 and YJJ432 (Fig. 3b). In SCRaMbLEd strain YJJ168,
220 the upregulated genes ERG24, ERG25, ERG26 and ERG27 were involved in ergosterol

221 biosynthesis, while ERG10, ERG20 and BTS1 were involved in terpenoid backbone
222 biosynthesis. In YJJ432, ERG24, ERG26 and ERG27, which are involved in the
223 biosynthesis of ergosterol, and ERG10, ERG12, ERG20 and BTS1, which are involved
224 in terpenoid backbone biosynthesis, were found to be upregulated. As a consequence,
225 these two pathways could increase the flux of the MVA pathway and cell storage
226 capacity of hydrophobic carotenoids[37, 38]. The improvement of citrate cycle could
227 provide sufficient reducing power and energy for the MVA pathway. These
228 transcriptome analyses indicated that the improved yield of astaxanthin was caused by
229 the upregulation of these genes, further clarifying the direct effect of the SVs on
230 astaxanthin accumulation. The results demonstrated the SVs can led to large
231 reorganization of the genetic information along the chromosomes and accelerate the
232 directed genome evolution with selection of targeted phenotypes.
233

234 **Rational introduction of inversion and translocation in yeast**

235 To verify the effect of the pericentric inversion and trans-chromosomic translocation,
236 we developed a method to rationally generate these inversions and translocations. First,
237 we constructed an astaxanthin-producing strain named YJJ468 from the wild-type
238 strain BY4741 by integrating the biosynthesis pathway of astaxanthin at the
239 *YEL063C*/*CAN1* locus of chromosome V. Then, we designed an on/off switch
240 consisting of two markers (URA3 and Hyg). As shown in Fig. 4a, the URA3 promoter
241 was inserted upstream of loxP site 1, and the open reading frame of URA3 was inserted
242 downstream of loxP site 1, allowing the expression of URA3. Hyg without a promoter

243 was positioned immediately downstream of loxP site 2. A complete HIS3 marker was
244 positioned upstream of loxP site 2 as a selection marker to help loxP-Hyg integrate into
245 the chromosome. The pGal1-Cre-EBD-tCYC1 plasmid with a G418 marker was
246 transformed into strain YJJ468 (Supplementary Fig. 7). The activation of Cre
247 recombinase will catalyze the recombination of the two loxP sites, leading to a change
248 in the phenotype of the yeast from Hyg- to Hyg+. Consequently, hygromycin media
249 could be used to select translocation and inversion strains. Using the above approach,
250 strain YJJ473 with pericentric inversion and strain YJJ474 with trans-chromosomic
251 translocation were generated and isolated by screening on SC-hygromycin agar plates.
252 Strains YJJ473 and YJJ474 were further analyzed using whole-genome sequencing to
253 verify the genomic variations produced by the recombination. As Fig. 4a shows, the
254 inversion and translocation region had breakpoints at the loxP sites in YJJ473 and
255 YJJ474, indicating that the desired inversion and translocation were artificially
256 recreated from the wild-type strain YJJ468.
257 Meanwhile, PCR was used to further verify the inversion and translocation. Before
258 recombination, sequences in YJJ468 could be amplified by primer pairs 1/2, 3/4, 5/6,
259 and 7/8. After recombination, sequences in YJJ473 could be amplified by primer pairs
260 1/3 and 2/4, while sequences in YJJ474 could be amplified by primer pairs 5/8 and 6/7
261 (Fig. 4b). Therefore, we can confirm that inversion and translocation events occurred
262 in YJJ473 and YJJ474. Compared to the initial strain yJJ468, YJJ473 and YJJ474 had
263 enhanced astaxanthin production phenotypes, yielding 1.11 mg/g DCW and 1.28 mg/g
264 DCW, respectively, which were similar to those of the SCRaMbLEd strains (Fig. 4c).

YJJ473 and YJJ474 increased the astaxanthin yield 1.8- and 2.1-fold relative to the parent strain YJJ468. These results indicated that the YJL052C-A-YJR071C inversion and YJR130C-YER164W translocation increased the production of astaxanthin and were responsible for the enhanced astaxanthin production phenotypes of SCRaMbLE strains yJJ168 and yJJ432. The results indicated that the YJL052C-A-YJR071C inversion and YJR130C-YER164W translocation contributed to the improvement of astaxanthin production. It is anticipated that we can used the model learned from the random screen of SCRaMbLE and successfully harnessed the precise introduction of pericentric inversions and trans-chromosomic translocation by rational design.

Discussion

Our study focused on investigating complex chromosome SVs by enabling haploid yeast containing multiple synthetic chromosomes to be SCRaMbLEd, which has significant advantages over pre-existing methods for laboratory evolution. First, traditional evolution approaches, such as physical mutagenesis or chemical mutagenesis, typically cause hundreds of single nucleotide polymorphisms (SNPs) or insertions and deletions (indels)[39], which make it difficult to confirm the targets responsible for observed changes in phenotypes. In comparison, SCRaMbLE has been demonstrated to rapidly generate larger scale SVs, providing clear targets to verify and understand more deeply. In this study, we have demonstrated that pathway-doubling is not the only way to increase yield [17], changes in map position and direction of endogenous genes can also affect yield. Second, the synthetic yeast project (Sc2.0) aims

287 to synthesize 16 yeast chromosomes, each of which contains hundreds of loxPsym sites,
288 downstream of every nonessential gene. Our research has shown that SCRaMbLE with
289 two synthetic chromosomes can generate translocations between two synthetic
290 chromosomes. Thus, it is anticipated that the integration of multiple synthetic
291 chromosomes will extend the diversity and quantity of SVs. Moreover, SCRaMbLE
292 with multiple synthetic chromosomes provided a powerful model in which to
293 investigate the trajectory of chromosome SVs during iterative evolution. In this study,
294 YJJ432 not only inherited the inversion spanning the centromere from YJJ168 but also
295 acquired new genetic changes, namely, a translocation between two synthetic
296 chromosomes.
297
298 The SCRaMbLE system provided sufficiently large structural variations to allow us to
299 analyze novel interactions and structures via Hi-C technology. The translocation strain
300 YJJ474 on the right arm of synV (YJR130C) has a closer spatial distance with synX
301 and consequently has stronger interactions. Chromosomal SVs cause changes in the 3D
302 architecture of the genome and potentially alter cellular functions. The development of
303 the 3C technique and its derivatives has provided a toolbox that enables the systematic
304 spatial interrogation of multiple loci or even the entire genome[40, 41]. Based on
305 genome-wide high-throughput chromosome conformation capture (Hi-C) technology,
306 a 2D heat map can be constructed to indicate the frequency of interaction between two
307 points in the genome. Depending on their positions, SVs often change the Hi-C profile
308 of a locus, leaving specific signatures that can be analyzed further[42, 43]. For example,

309 deletions can result in novel interactions between two regions that were previously
310 separated, whereas inversions result in a characteristic 'bow tie' configuration when
311 mapped onto a reference genome. Furthermore, owing to its proximity-ligation nature,
312 the Hi-C is also suitable for the identification of SVs without a priori knowledge[43-
313 46].
314
315 SCRaMbLEing two synthetic chromosomes generated random and complex SVs,
316 which reshaped chromosomes 3D architecture. Duan.et al reported that the genome 3D
317 structure affected genes expressions[47] It is known that telomeres and centromeres
318 could inhibit the expression of genes nearby [48], while the autonomously replicating
319 sequence (ARS) could increase the expression of genes nearby[49]. In the study, the
320 pericentric inversions and trans-chromosomes translocation changed the map position
321 of centromeres in chromosome X and caused the exchange of the right telomeres of
322 chromosome V with chromosome X, respectively. Thus, larger number of genes
323 position and the transcription direction, which affected the transcription levels of genes
324 in the regions nearby the breakpoint of SVs. It is demonstrated that over-expression of
325 YJR086W(STE18), YJR123W(RPS5) and YJR135C(MCM22) improved astaxanthin
326 yield. Choudhury.et al show that phosphorylation of the yeast Gg subunit (Ste18) can
327 serve as intrinsic regulators of G protein signaling and differentially activates mitogen-
328 activated protein kinases (MAPKs) pathway [50], which potentially mediates the
329 activation of some transcription factors and metabolic network related to the
330 astaxanthin biosynthesis. Ghosh.et al reported Rps5 is an essential gene coding a

protein component of the small (40S) ribosomal subunit. Over-expression of Rps5 potentially impact the translation initiation of yeast S. cerevisiae [51], which may increase the translation of some genes being beneficial to the astaxanthin biosynthesis. Poddar.et al demonstrated MCM22 involved in chromosome segregation, mutations of which caused a decrease in the stability of the minichromosome [52]. Over-expression of MCM22 potentially maintained the stability of chromosome during segregation and enhanced the cell viability during fermentation. The exact mechanism of over-expression of STE18, RPS5 and MCM22 contributing to astaxanthin biosynthesis is unknown, however, upregulation of these genes may be beneficial for tuning metabolic network, the translation initiation process and stability of chromosome during segregation, which may explain why this genes affects astaxanthin biosynthesis.

In this manuscript, we have developed both a random method and a rational method to generate complex SVs. The random method uses SCRaMbLE in yeast with two synthetic chromosomes to generate yeast libraries containing complex SVs for screening desired phenotypes. The rational method enables a selection marker to switch from transcriptionally “off” to transcriptionally “on”. The rational method provides a convenient way to determine the effects of translocation and inversion targets on strain phenotypes. In addition, inversion and translocation strains generated from wild-type strains can be used as materials to study open genetic questions, such as whether inversion and translocation strains become reproductively isolated from control strains. By this method, we validated a larger fragment translocation (right arm of synV

(YJR130C) and right arm of synX (YER164W)) and an inversion (YJL052C-A-YJR071C) in wild-type strains and found that both the translocation and inversion increased the yield of astaxanthin. This strategy is potentially a powerful tool for inducing the recombination of any two positions on chromosomes. How nature evolves with great biodiversity and nurtures organisms containing various numbers of chromosomes is not known. Our work may spark interest and provide a new handle for researchers to study this fundamental biological problem.

363 ## Methods

364 **Strains and media.**

365 All yeast strains used in this study are described in Table 1. The strain SYNVX carries
366 a synV, and a synX is derived from BY4741 (*MATa leu2Δ0 met15Δ0 ura3Δ0 his3Δ1*).
367 BY4741 was used as the initial strain to reconstruct the translocations and inversions
368 caused by SCRaMbLE of the strains and verify targets of astaxanthin yield
369 improvement.

370 Yeast strains were cultured in YPD medium (10 g l^{-1} yeast extract, 20 g l^{-1} peptone,
371 and 20 g l^{-1} glucose). SGal-Ura (synthetic media lacking uracil with 20 g l^{-1} galactose)
372 with 1 μM β-estradiol was used to induce SCRaMbLE. SC medium containing 1 g L−1
373 5-FOA was used to screen strains without the URA3 marker. All yeast solid media
374 contained 20 g L−1 agar. β-Estradiol and 5-FOA were purchased from Sigma-Aldrich.
375 *E. coli* DH5α purchased from BEIJING Biomed Co., Ltd. was used for plasmid
376 construction and replication. *E. coli* were cultivated at 37 °C in Luria–Bertani (LB)
377 complete medium. Kanamycin (50 μg/mL) or ampicillin (100 μg/mL) was added to the
378 medium for selection.

379

380 **Construction of plasmids and strains.**

381 YJJ001 (astaxanthin-producing control strain) was constructed by homologous
382 recombination in SYNVX, directed by 500-bp CAN1 and 500-bp delta site genomic
383 sequences flanking crtE-crtI-crtYB-crtZ-crtW-LEU2. YJJ002 was constructed by
384 transforming YJJ001 with pCRE4 (Supplementary Fig. 1, Supplementary Data 2),

385 followed by selection on SC-URA agar. Overexpression plasmids were constructed by
386 Gibson assemble. The gene knockout cassette (left homologous arm-URA3-right
387 homologous arm) was assembled by overlap extension PCR (OE-
388 PCR).Transformations were performed using the standard lithium acetate
389 procedure[53].
390
391 **SCRaMbLE.**
392 YJJ002 containing the inducible Cre plasmid pGal1-Cre-EBD-tCYC1 was grown
393 overnight in 5 mL SC-Ura media (30 °C, 250 r.p.m. shaking). Then, the cells were
394 harvested and washed three times with sterile water to wash out glucose, and the culture
395 was diluted to an OD600 of 0.6-1.0 in 3 mL SGal-Ura medium. Then, 1 μmol L^{-1} β-
396 estradiol was added to the cultures to induce SCRaMbLE for 6 h (30 °C, 250 r.p.m.
397 shaking). Cells were washed twice by centrifugation, resuspended in sterile water,
398 diluted 5,000-fold, and plated on SC-Ura. The plates were incubated at 30 °C for 60 h.
399
400 **HPLC analysis of astaxanthin production.**
401 SCRaMbLE strains with darker colors were selected for fermentation in shake flasks.
402 Three independent colonies of each strain were inoculated into 5 ml of YPD medium
403 and grown at 30 °C until the OD 600≈ 8.0 (approximately 24 h). Then, the seed culture
404 was transferred into 50 mL fresh YPD with 40 g l^{-1} glucose medium at an initial OD
405 600 of 0.1 and grown until ready to harvest.
406 Astaxanthin was extracted from HCl–heat treated cells with acetone according to Zhou

407 et al. [54] and Wang et al. [35] . Carotenoids were extracted as described below. Cells
408 from 2 mL culture were collected and washed with distilled water. Then, the cells were
409 resuspended in 1 mL of 3 M HCl, boiled for 5 min, and subsequently cooled in an ice
410 bath for 5 min. After that, the cell debris was washed twice with distilled water and
411 resuspended in 0.5 mL of acetone containing 1% (wv^{-1}) butylated hydroxytoluene.
412 Then, the mixture was vortexed until colorless (approximately 20 min) and incubated
413 at 30 °C for 10 min. This was followed by centrifugation at 12,000 rpm for 5 min. The
414 acetone phase containing the extracted astaxanthin was filtered through a 0.22-μm
415 membrane for HPLC analysis.
416
417 **PCRTags analysis.**
418 All the synV and synX PCRTags involved in this study are listed in Supplementary
419 Table 2. Amplification of PCRTags was performed using 7.5 μL 2 × Rapid Taq Master
420 Mix (Vazyme Biotech Co., Ltd), 0.4 μL each of forward and reverse primers, 1 μL
421 genomic DNA, and 5.7 μL ddH2O. The reaction procedure was as follows: 95 °C/1 min,
422 35 cycles of 95 °C/20 s, 53 °C/20 s, 72 °C/15 s and a final extension of 72 °C/5 min.
423 Detection of PCRTags was performed by gel electrophoresis.
424
425 **Whole-genome sequencing (WGS) and analysis.**
426 WGS was performed at BGI (Beijing Genomic Institute in Shenzhen, China), and cells
427 were harvested at exponential phase. Libraries were prepared and analyzed using an
428 Illumina HiSeq X-Ten system. The sequencing data were filtered with SOAPnuke

429 (v1.5.2)[55]. and clean reads were stored in FASTQ format for downstream analysis.
430 The read comparison was performed using BWA software with the reference sequence.
431 SVs including insertions, deletions, inversions, intrachromosomal translocations, and
432 interchromosomal translocations were detected using Break Dancer software.
433
434 **Transcriptional analysis.**
435 Yeast cells were harvested from YPD medium at 24 h (exponential phase). Total RNA
436 was extracted using the TRIzol® method following the NEB Next Ultra™ RNA
437 protocol. The concentration of the extracted RNA samples was determined using a
438 NanoDrop system (NanoDrop, Madison, USA), and the integrity of the RNA was
439 examined based on the RNA integrity number (RIN) determined using an Agilent 2100
440 Bioanalyzer (Agilent, Santa Clara, USA). RNA sequencing was carried out by the
441 BGISeq500 platform (BGI-Shenzhen, China). The sequencing data were filtered with
442 SOAPnuke (v1.5.2).[55]
443 Clean reads were obtained and stored in FASTQ format. The clean reads were mapped
444 to the reference genome using HISAT2 (v2.0.4)[56]. Bowtie2 (v2.2.5)[57] was applied
445 to align the clean reads to the reference coding gene set, and the expression level of
446 each gene was calculated by RSEM (v1.2.12)[58]. The heatmap of the gene expression
447 in different samples was drawn by GraphPad Prism (v8.0.1). Essentially, differential
448 expression analysis was performed using DESeq2 (v1.4.5)[59] with a Q value $\leqslant$ 0.05.
449 To gain insight into the change in phenotype, GO (http://www.geneontology.org/) and
450 KEGG (https://www.kegg.jp/) enrichment analyses of annotated differentially

451 expressed genes were performed by Phyper
452 (https://en.wikipedia.org/wiki/Hypergeometric_distribution) based on the
453 hypergeometric test. Significant terms and pathways were identified as those with
454 Bonferroni-corrected *P*-values below a rigorous threshold (*P*-value ≤ 0.05). Triplicate
455 samples were used for transcriptional analysis. The Saccharomyces Genome Database
456 (SGD)[60] was used to obtain gene information.
457
458 **Hi-C library generation and sequencing.**
459 Hi-C library generation and sequencing were carried out by Frasergen (Wuhan, China),
460 and cells were harvested at exponential phase. Cells were resuspended in 1×PBS to an
461 OD600 of 1.0. Cells were cross-linked in a 3% final concentration of fresh
462 formaldehyde and quenched with glycine (0.15 M final concentration) for 5 min. The
463 cells were resuspended in 1 mL of 1× NEBuffer 2.1 (NEB) and homogenized by
464 grinding to a fine powder in liquid nitrogen. Then, the homogenized yeast material was
465 washed with 25 mL of 1× NEBuffer 2.1 and suspended in 2.5 mL of 1× NEBuffer 2.1.
466 Cells were split into aliquots (V =456 μL) and solubilized in 0.1% SDS for 10 min at
467 65 °C. Cross-linked DNA was digested with 200 U MboI (NEB) per tube at 37 °C
468 overnight. Restriction fragment ends were labeled with biotinylated cytosine
469 nucleotides by biotin-14-dCTP (TriLINK). Blunt-end ligation was carried out at 16 °C
470 overnight in the presence of 100 Weiss units of T4 DNA ligase (Thermo, 10.0 mL final
471 volume per tube).
472 DNA purification was achieved through overnight incubation at 65 °C with 200 μg/mL

473 proteinase K (Thermo). Purified DNA was sheared to a length of ~400 bp. Point ligation
474 junctions were pulled down by Dynabeads® MyOne™ Streptavidin C1 (Thermo
475 Fisher). The Hi-C library for Illumina sequencing was prepared using the NEBNext®
476 Ultra™ II DNA library Prep Kit for Illumina (NEB) according to the manufacturer's
477 instructions. Fragments of between 400 and 600 bp were paired-end sequenced on an
478 Illumina HiSeq X10 platform (San Diego, CA, United States) in 150PEmode. Two
479 replicates were generated for each group of materials.
480

481 **Construction of contact map.**

482 The contact maps were generated using the ICE software package (version
483 1f8815d0cc9e)[61], and the Hi-C data of YJJ001, YJJ168 and YJJ432 cells were
484 iteratively mapped to their own genomes. Dangling ends and other unusable data were
485 filtered out, and the valid pairs were binned into 10 kb nonoverlapping genomic
486 intervals to generate contact maps. The contact maps were normalized using an iterative
487 normalization method to eliminate systematic biases.
488

489 **Cre/loxP induced chromosome translocation and inversion.**

490 Translocations and inversions were detected in YJJ168 and YJJ432 and verified in the
491 wild-type strain BY4741 by introducing two Cre/loxP sites to the corresponding
492 position. LoxP sites were integrated by homologous recombination. Homologous arms
493 upstream and downstream were amplified from the genome of BY4741. Two loxP sites
494 (loxP site 1 and loxP site 2) were integrated along with URA3+ and HIS3+/Hyg- as

495 selection markers. The URA3 promoter was inserted upstream of loxP site 1, and open
496 reading frames of URA3 were inserted downstream of the loxP site, allowing the
497 expression of URA3. Hyg without a promoter was positioned adjacent to downstream
498 loxP site 2 and the HIS3 promoter, and open reading frames of HIS3 were positioned
499 upstream of loxP site 2. Adding 1 μmol L–1 β-estradiol to the cultures to switch on Cre-
500 mediated recombination between the two loxP sites results in translocation and
501 inversion, which subsequently turn on the expression of the Hyg gene and
502 simultaneously shut down URA3 expression. Translocation and inversion strains could
503 be selected on SC-LEU-5-FOA plates and SC-LEU+Hyg.
504

505 **Acknowledgements**
506 This work was funded by Ministry of science and technology the National Key
507 Research and Development Program of China (2021YFC2100800), and the National
508 Natural Science Foundation of China (31800719, 31861143017 and 21621004).

509 **Author contributions**
510 B.J., and J.J. contributed equally to this work. B.J., J.J., and Y.J.Y. designed the
511 experiments. B.J., J.J., and M.Z.H performed the experiments. B.J., J.J., and Y.J.Y.
512 wrote the manuscript and all authors edited the manuscript. This project was supervised
513 by Y.J.Y.

514 **Conflict of Interest**
515 The authors declare no competing financial interests.

516 **Reference**

517 1. Dujon B, Sherman D, Fischer G, Durrens P, Casaregola S, Lafontaine I, De Montigny J,
518 Marck C, Neuvéglise C, Talla E, et al: Genome evolution in yeasts. *Nature* 2004, 430:35-
519 44.
520 2. Redon R, Ishikawa S, Fitch KR, Feuk L, Perry GH, Andrews TD, Fiegler H, Shapero MH,
521 Carson AR, Chen WW, et al: Global variation in copy number in the human genome.
522 *Nature* 2006, 444:444-454.
523 3. Kidd JM, Cooper GM, Donahue WF, Hayden HS, Sampas N, Graves T, Hansen N, Teague
524 B, Alkan C, Antonacci F, et al: Mapping and sequencing of structural variation from eight
525 human genomes. *Nature* 2008, 453:56-64.
526 4. Dujon B: Yeast evolutionary genomics. *Nature Reviews Genetics* 2010, 11:512-524.
527 5. Peter J, De Chiara M, Friedrich A, Yue JX, Pflieger D, Bergstrom A, Sigwalt A, Barre B,
528 Freel K, Llored A, et al: Genome evolution across 1,011 Saccharomyces cerevisiae
529 isolates. *Nature* 2018, 556:339-+.
530 6. Conrad DF, Pinto D, Redon R, Feuk L, Gokcumen O, Zhang YJ, Aerts J, Andrews TD,
531 Barnes C, Campbell P, et al: Origins and functional impact of copy number variation in
532 the human genome. *Nature* 2010, 464:704-712.
533 7. Pang AW, MacDonald JR, Pinto D, Wei J, Rafiq MA, Conrad DF, Park H, Hurles ME, Lee C,
534 Venter JC, et al: Towards a comprehensive structural variation map of an individual
535 human genome. *Genome Biology* 2010, 11.
536 8. Darling AE, Miklos I, Ragan MA: Dynamics of Genome Rearrangement in Bacterial
537 Populations. *Plos Genetics* 2008, 4:16.
538 9. Yue JX, Li J, Aigrain L, Hallin J, Persson K, Oliver K, Bergstrom A, Coupland P, Warringer J,

539 Lagomarsino MC, et al: Contrasting evolutionary genome dynamics between
540 domesticated and wild yeasts. *Nature Genetics* 2017, 49:913-+.
541 10. Pevzner P, Tesler G: Genome Rearrangements in mammalian evolution: Lessons from
542 human and mouse genomes. *Genome Research* 2003, 13:37-45.
543 11. Henssen AG, Koche R, Zhuang J, Jiang E, Reed C, Eisenberg A, Still E, MacArthur IC,
544 Rodriguez-Fos E, Gonzalez S, et al: PGBD5 promotes site-specific oncogenic mutations
545 in human tumors. *Nature Genetics* 2017, 49:1005-+.
546 12. Fleiss A, O'Donnell S, Fournier T, Lu W, Agier N, Delmas S, Schacherer J, Fischer G:
547 Reshuffling yeast chromosomes with CRISPR/Cas9. *PLoS Genet* 2019, 15:e1008332.
548 13. Selmecki AM, Maruvka YE, Richmond PA, Guillet M, Shoresh N, Sorenson AL, De S,
549 Kishony R, Michor F, Dowell R, Pellman D: Polyploidy can drive rapid adaptation in yeast.
550 *Nature* 2015, 519:349-352.
551 14. Li Y, Wu Y, Ma L, Guo Z, Xiao W, Yuan Y: Loss of heterozygosity by SCRaMbLEing.
552 *Science China Life Sciences* 2019, 62:381-393.
553 15. Eyupoglu D, Bozkurt S, Haznedaroglu I, Buyukasik Y, Guven D: The Impact of Variant
554 Philadelphia Chromosome Translocations on the Clinical Course of Chronic Myeloid
555 Leukemia. *Turkish Journal of Hematology* 2016, 33:60-65.
556 16. Nishikawa M, Ichiyama T, Hayashi T, Furukawa S: Mobius-like syndrome associated with
557 a 1;2 chromosome translocation. *Clinical genetics* 1997, 51:122-123.
558 17. Sotoudeh A, Rostami P, Nakhaeimoghadam M, Mohsenipour R, Rezaei N: Pericentric
559 Inversion of Chromosome 9 in an Infant With Ambiguous Genitalia. *Acta medica Iranica*
560 2017, 55:655-657.

561 18. Puddu F, Herzog M, Selivanova A, Wang SY, Zhu J, Klein-Lavi S, Gordon M, Meirman R,
562 Millan-Zambrano G, Ayestaran I, et al: Genome architecture and stability in the
563 Saccharomyces cerevisiae knockout collection. *Nature* 2019, 573:416-+.
564 19. Natesuntorn W, Iwami K, Matsubara Y, Sasano Y, Sugiyama M, Kaneko Y, Harashima S:
565 Genome-wide construction of a series of designed segmental aneuploids in
566 Saccharomyces cerevisiae. *Scientific Reports* 2015, 5.
567 20. Si T, Xiao H, Zhao H: Rapid prototyping of microbial cell factories via genome-scale
568 engineering. *Biotechnol Adv* 2015, 33:1420-1432.
569 21. Jia B, Wu Y, Li B-Z, Mitchell LA, Liu H, Pan S, Wang J, Zhang H-R, Jia N, Li B, et al: Precise
570 control of SCRaMbLE in synthetic haploid and diploid yeast. *Nature Communications*
571 2018, 9.
572 22. Wu Y, Zhu R-Y, Mitchell LA, Ma L, Liu R, Zhao M, Jia B, Xu H, Li Y-X, Yang Z-M, et al: In
573 vitro DNA SCRaMbLE. *Nature Communications* 2018, 9.
574 23. Shen MJ, Wu Y, Yang K, Li Y, Xu H, Zhang H, Li B-Z, Li X, Xiao W-H, Zhou X, et al:
575 Heterozygous diploid and interspecies SCRaMbLEing. *Nature Communications* 2018, 9.
576 24. Luo Z, Wang L, Wang Y, Zhang W, Guo Y, Shen Y, Jiang L, Wu Q, Zhang C, Cai Y, Dai J:
577 Identifying and characterizing SCRaMbLEd synthetic yeast using ReSCuES. *Nature*
578 *Communications* 2018, 9.
579 25. Blount BA, Gowers GOF, Ho JCH, Ledesma-Amaro R, Jovicevic D, McKiernan RM, Xie ZX,
580 Li BZ, Yuan YJ, Ellis T: Rapid host strain improvement by in vivo rearrangement of a
581 synthetic yeast chromosome. *Nature Communications* 2018, 9.
582 26. Wang J, Jia B, Xie ZX, Li YX, Yuan YJ: Improving prodeoxyviolacein production via

583 multiplex SCRaMbLE iterative cycles. *Frontiers of Chemical Science and Engineering*
584 2018, 12:806-814.
585 27. Ma L, Li Y, Chen X, Ding M, Wu Y, Yuan Y-J: SCRaMbLE generates evolved yeasts with
586 increased alkali tolerance. *Microbial Cell Factories* 2019, 18.
587 28. Liu W, Luo Z, Wang Y, Pham NT, Tuck L, Pérez-Pi I, Liu L, Shen Y, French C, Auer M, et
588 al: Rapid pathway prototyping and engineering using in vitro and in vivo synthetic
589 genome SCRaMbLE-in methods. *Nature Communications* 2018, 9.
590 29. Gowers GOF, Chee SM, Bell D, Suckling L, Kern M, Tew D, McClymont DW, Ellis T:
591 Improved betulinic acid biosynthesis using synthetic yeast chromosome recombination
592 and semi-automated rapid LC-MS screening. *Nature Communications* 2020, 11.
593 30. Akdemir KC, Le VTT, Chandran S, Li YL, Verhaak RG, Beroukhim R, Campbell PJ, Chin L,
594 Dixon JR, Futreal PA, et al: Disruption of chromatin folding domains by somatic genomic
595 rearrangements in human cancer. *Nature Genetics* 2020, 52:294-+.
596 31. Xie ZX, Li BZ, Mitchell LA, Wu Y, Qi X, Jin Z, Jia B, Wang X, Zeng BX, Liu HM, et al:
597 "Perfect" designer chromosome V and behavior of a ring derivative. *Science* 2017, 355:8.
598 32. Wu Y, Li BZ, Zhao M, Mitchell LA, Xie ZX, Lin QH, Wang X, Xiao WH, Wang Y, Zhou X, et
599 al: Bug mapping and fitness testing of chemically synthesized chromosome X. *Science*
600 2017, 355:7.
601 33. Ambati RR, Phang SM, Ravi S, Aswathanarayana RG: Astaxanthin: Sources, Extraction,
602 Stability, Biological Activities and Its Commercial Applications-A Review. *Marine Drugs*
603 2014, 12:128-152.
604 34. Igielska-Kalwat J, Goscianska J, Nowak I: Carotenoids as natural antioxidants. *Postepy*

605 *higieny i medycyny doswiadczalnej (Online)* 2015, 69:418-428.

606 35. Wang R, Gu X, Yao M, Pan C, Liu H, Xiao W, Wang Y, Yuan Y: Engineering of β-carotene
607 hydroxylase and ketolase for astaxanthin overproduction in Saccharomyces cerevisiae.
608 *Frontiers of Chemical Science and Engineering* 2017, 11:89-99.

609 36. Wu X-L, Li B-Z, Zhang W-Z, Song K, Qi H, Dai J-b, Yuan Y-J: Genome-wide landscape
610 of position effects on heterogeneous gene expression in Saccharomyces cerevisiae.
611 *Biotechnology for Biofuels* 2017, 10.

612 37. Wu T, Ye LJ, Zhao DD, Li SW, Li QY, Zhang BL, Bi CH, Zhang XL: Membrane engineering
613 - A novel strategy to enhance the production and accumulation of beta-carotene in
614 Escherichia coli. *Metabolic Engineering* 2017, 43:85-91.

615 38. Gao SL, Tong YY, Zhu L, Ge M, Zhang YA, Chen DJ, Jiang Y, Yang S: Iterative integration
616 of multiple-copy pathway genes in Yarrowia lipolytica for heterologous beta-carotene
617 production. *Metabolic Engineering* 2017, 41:192-201.

618 39. Jin J, Wang Y, Yao M, Gu X, Li B, Liu H, Ding M, Xiao W, Yuan Y: Astaxanthin
619 overproduction in yeast by strain engineering and new gene target uncovering.
620 *Biotechnology for Biofuels* 2018, 11.

621 40. Lieberman-Aiden E, van Berkum NL, Williams L, Imakaev M, Ragoczy T, Telling A, Amit I,
622 Lajoie BR, Sabo PJ, Dorschner MO, et al: Comprehensive Mapping of Long-Range
623 Interactions Reveals Folding Principles of the Human Genome. *Science* 2009, 326:289-
624 293.

625 41. Dekker J, Marti-Renom MA, Mirny LA: Exploring the three-dimensional organization of
626 genomes: interpreting chromatin interaction data. *Nature Reviews Genetics* 2013,

627 14:390-403.

628 42. Bianco S, Lupianez DG, Chiariello AM, Annunziatella C, Kraft K, Schopflin R, Wittler L,
629 Andrey G, Vingron M, Pombo A, et al: Polymer physics predicts the effects of structural
630 variants on chromatin architecture. *Nature Genetics* 2018, 50:662-+.

631 43. Burton JN, Adey A, Patwardhan RP, Qiu RL, Kitzman JO, Shendure J: Chromosome-scale
632 scaffolding of de novo genome assemblies based on chromatin interactions. *Nature*
633 *Biotechnology* 2013, 31:1119-+.

634 44. Rickman DS, Soong TD, Moss B, Mosquera JM, Dlabal J, Terry S, MacDonald TY, Tripodi
635 J, Bunting K, Najfeld V, et al: Oncogene-mediated alterations in chromatin
636 conformation. *Proceedings of the National Academy of Sciences of the United States of*
637 *America* 2012, 109:9083-9088.

638 45. Harewood L, Kishore K, Eldridge MD, Wingett S, Pearson D, Schoenfelder S, Collins VP,
639 Fraser P: Hi-C as a tool for precise detection and characterisation of chromosomal
640 rearrangements and copy number variation in human tumours. *Genome Biology* 2017,
641 18:11.

642 46. Rao SSP, Huntley MH, Durand NC, Stamenova EK, Bochkov ID, Robinson JT, Sanborn AL,
643 Machol I, Omer AD, Lander ES, Aiden EL: A 3D Map of the Human Genome at Kilobase
644 Resolution Reveals Principles of Chromatin Looping. *Cell* 2014, 159:1665-1680.

645 47. Duan Z, Andronescu M, Schutz K, McIlwain S, Kim YJ, Lee C, Shendure J, Fields S, Blau
646 CA, Noble WS: A three-dimensional model of the yeast genome. *Nature* 2010, 465:363-
647 367.

648 48. Chen X, Zhang J: The Genomic Landscape of Position Effects on Protein Expression Level

649 and Noise in Yeast. *Cell Syst* 2016, 2:347-354.

650 49. Flagfeldt DB, Siewers V, Huang L, Nielsen J: Characterization of chromosomal integration
651 sites for heterologous gene expression in Saccharomyces cerevisiae. *Yeast* 2009, 26:545-
652 551.

653 50. Choudhury S, Baradaran-Mashinchi P, Torres MP: Negative Feedback Phosphorylation
654 of Ggamma Subunit Ste18 and the Ste5 Scaffold Synergistically Regulates MAPK
655 Activation in Yeast. *Cell Rep* 2018, 23:1504-1515.

656 51. Saliba AE, Westermann AJ, Gorski SA, Vogel J: Single-cell RNA-seq: advances and future
657 challenges. *Nucleic Acids Res* 2014, 42:8845-8860.

658 52. MCM21and MCM22, two novel genes of the yeast Saccharomyces cerevisiae are
659 required for chromosome transmission.

660 53. Gietz RD, Schiestl RH, Willems AR, Woods RA: Studies on the transformation of intact
661 yeast cells by the LiAc/SS-DNA/PEG procedure. *Yeast (Chichester, England)* 1995,
662 11:355-360.

663 54. Zhou PP, Ye LD, Xie WP, Lv XM, Yu HW: Highly efficient biosynthesis of astaxanthin in
664 Saccharomyces cerevisiae by integration and tuning of algal crtZ and bkt. *Applied*
665 *Microbiology and Biotechnology* 2015, 99:8419-8428.

666 55. Li RQ, Li YR, Kristiansen K, Wang J: SOAP: short oligonucleotide alignment program.
667 *Bioinformatics* 2008, 24:713-714.

668 56. Kim D, Landmead B, Salzberg SL: HISAT: a fast spliced aligner with low memory
669 requirements. *Nature Methods* 2015, 12:357-U121.

670 57. Langmead B, Salzberg SL: Fast gapped-read alignment with Bowtie 2. *Nature Methods*

671 2012, 9:357-U354.

672 58. Li B, Dewey CN: RSEM: accurate transcript quantification from RNA-Seq data with or

673 without a reference genome. *Bmc Bioinformatics* 2011, 12:16.

674 59. Love MI, Huber W, Anders S: Moderated estimation of fold change and dispersion for

675 RNA-seq data with DESeq2. *Genome Biology* 2014, 15:38.

676 60. Cherry JM, Hong EL, Amundsen C, Balakrishnan R, Binkley G, Chan ET, Christie KR,

677 Costanzo MC, Dwight SS, Engel SR, et al: Saccharomyces Genome Database: the

678 genomics resource of budding yeast. *Nucleic Acids Research* 2012, 40:D700-D705.

679 61. Imakaev M, Fudenberg G, McCord RP, Naumova N, Goloborodko A, Lajoie BR, Dekker J,

680 Mirny LA: Iterative correction of Hi-C data reveals hallmarks of chromosome

681 organization. *Nature Methods* 2012, 9:999-+.

682 62. Brachmann CB, Davies A, Cost GJ, Caputo E, Li J, Hieter P, Boeke JD: Designer deletion

683 strains derived from Saccharomyces cerevisiae S288C: a useful set of strains and

684 plasmids for PCR-mediated gene disruption and other applications. *Yeast* 1998, 14:115-

685 132.

686

687

688 **Table 1 *S. cerevisiae* strains used in this study**

Strains	Description	Sources
BY4741	*MATa, HIS3Δ1, LEU2Δ0, MET15Δ0, URA3Δ0*	[62]
SYNVX	*MATa, HIS3Δ1, LEU2Δ0, MET15Δ0, URA3Δ0*	This study
YJJ001	yXZX573, CAN1:: astaxanthin pathway with Leu2 marker	This study
YJJ002	Introducing plasmid pGAL1-Cre-EBD-GFP-tCYC1 into strain YJJ001	This study
YJJ168	SCRaMbLEd strain from the YJJ002	This study
YJJ432	SCRaMbLEd strain from the YJJ168	This study
YJJ468	Astaxanthin producing strain, BY4741	This study
YJJ473	YJJ468 with inversion (YJL052C-A-YJR071C) strain	This study
YJJ474	YJJ468 with translocation (YJR130C and YER164W) strain	This study
YJJ522	YJJ001 with YJL053Woverexpression	This study
YJJ523	YJJ001 with YJL052C-A overexpression	This study
YJJ524	YJJ001 with YJL052W deletion	This study
YJJ525	YJJ001 with YJL049W overexpression	This study
YJJ526	YJJ001 with YJL046W overexpression	This study
YJJ527	YJJ001 with YJL045W overexpression	This study
YJJ528	YJJ001 with YJR067C overexpression	This study
YJJ529	YJJ001 with YJR068W overexpression	This study
YJJ530	YJJ001 with YJR070C overexpression	This study
YJJ531	YJJ001 with YJR071W overexpression	This study
YJJ532	YJJ001 with YJR072C overexpression	This study
YJJ533	YJJ001 with YJR076C overexpression	This study
YJJ534	YJJ001 with YJR079W overexpression	This study
YJJ535	YJJ001 with YJR080C overexpression	This study
YJJ536	YJJ001 with YJR082C overexpression	This study
YJJ537	YJJ001 with YJR085C overexpression	This study
YJJ538	YJJ001 with YJR086W overexpression	This study
YJJ539	YJJ001 with YJR087W overexpression	This study
YJJ540	YJJ001 with YJR088C overexpression	This study
YJJ541	YJJ001 with YER156C overexpression	This study
YJJ542	YJJ001 with YER158C deletion	This study
YJJ543	YJJ001 with YER163C overexpression	This study
YJJ544	YJJ001 with YER168C overexpression	This study
YJJ545	YJJ001 with YER170W overexpression	This study
YJJ546	YJJ001 with YJR122W overexpression	This study
YJJ547	YJJ001 with YJR123W overexpression	This study
YJJ548	YJJ001 with YJR127 deletion	This study
YJJ549	YJJ001 with YJR125C overexpression	This study
YJJ551	YJJ001 with YJR133W overexpression	This study
YJJ552	YJJ001 with YJR135C overexpression	This study
YJJ553	YJJ001 with YJR135W-A overexpression	This study
YJJ554	YJJ001 with YJR136C overexpression	This study

689

690 **Table 2** Known gene functions for beneficial over-expression

Gene	Description
YJR086W(STE18)	G protein gamma subunit; forms a dimer with Ste4p to activate the mating signaling pathway, forms a heterotrimer with Gpa1p and Ste4p to dampen signaling; C-terminus is palmitoylated and farnesylated, which are required for normal signaling
YJR123W(RPS5)	Protein component of the small (40S) ribosomal subunit; least basic of non-acidic ribosomal proteins; phosphorylated in vivo; essential for viability; homologous to mammalian ribosomal protein S5 and bacterial S7
YJR135C(MCM22)	Outer kinetochore protein and component of the Ctf3 subcomplex; binds to centromeric DNA in a Ctf19p-dependent manner; involved in chromosome segregation and minichromosome maintenance; orthologous to human centromere constitutive-associated network (CCAN) subunit CENP-K and fission yeast sim4

691

692

693

694

695

696

697

698 **Fig. 1 SCRaMbLE with two synthetic chromosomes generating complex SVs. a,**
699 **Schematic representation of structural variations in YJJ001, YJJ168 and YJJ432.**
700 **Synthetic chromosome V and synthetic chromosome X are abbreviated as synV**
701 **and synX, respectively. b, Normalized contact maps (bin size, 2 kb) of synthetic**
702 **chromosomes in three different strains: YJJ117, YJJ168 and YJJ432. All Hi-C**
703 **reads are mapped against the reference genome of the parental strain YJJ001. c,**
704 **Three-dimensional model of the YJJ001, YJJ168 and YJJ432 genomes. Synthetic**
705 **chromosomes and wild chromosomes are indicated with graduated color and gray,**
706 **respectively. The SV area are indicated with the dashed oval. d, The astaxanthin**
707 **yield of control strain YJJ001 and SCRaMbLEd strains YJJ168 and YJJ432.**
708

Fig. 2 Quantified interactions of loxP breakpoint-flanking regions. a, Triangle heat maps representing the contact frequencies among 20 bin regions (length 20 kb) upstream and downstream of two recombination sites (YJL052C-A and YJR071C) in YJJ168, labeled A, B, C, and D. Dots show fold changes in expression in the A, B, C, and D regions. b, Triangle heat maps representing the contact frequencies among 20 bin regions (length 20 kb) upstream and downstream of the two recombination sites (YER164W and YJR130C) in YJJ432, labeled E, F, G, and H. Dots show fold changes in expression in the E, F, G, H regions.

719

720 **Fig. 3 a, The astaxanthin yield of control strain YJJ001 and genes overexpression**

721 **and deletion around pericentric inversion strain breakpoint-flanking regions and**

722 **genes overexpression and deletion around trans-chromosomic translocation strain**

723 **breakpoint-flanking regions. (Student's t-test; *P < 0.05). b, Enrichment analysis**

724 **of transcriptomics of YJJ168 and YJJ432 were used to identify differentially**

725 **transcribed genes with known functions involved in KEGG pathways.**

726

727

728 **Fig. 4 Rational translocation and inversion of chromosomes. a, The process of**
729 **inversion and translocation was validated in wild-type strains. Wild-type**
730 **chromosome V and wild-type chromosome X are abbreviated as wt V and wt X,**
731 **respectively. Validation strains exhibited inversion and translocation events**
732 **between two LoxP sites. These events were identified by aligning all raw reads. b,**
733 **Verification of inversion and translocation by junction PCR. c, The astaxanthin**
734 **yield of the wild-type control strain YJJ468, inversion strain YJJ473 and**
735 **translocation strain YJJ474. Serial dilution assay of YJJ468, YJJ473, YJJ474.**

736

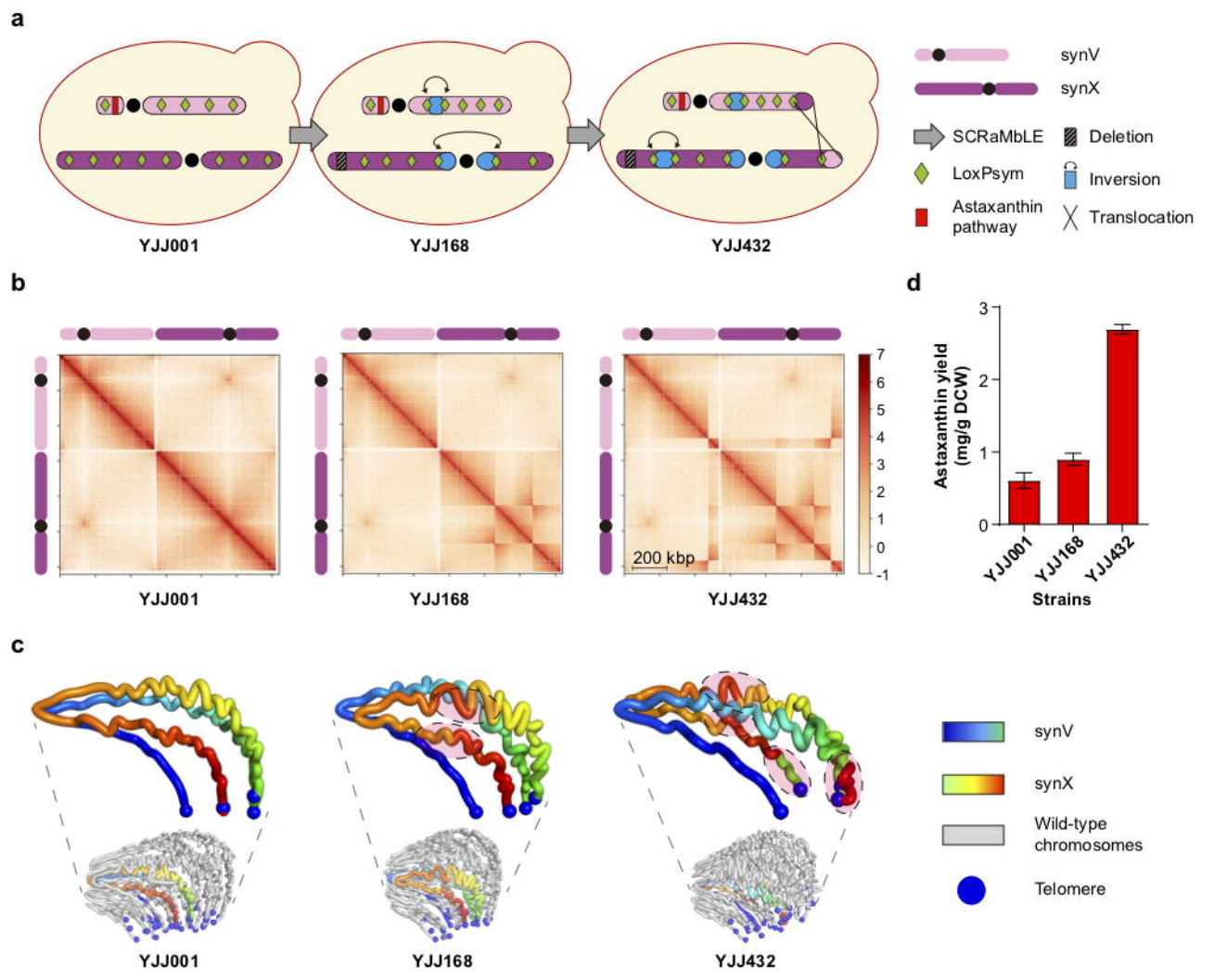
a
synV
synX
SCRaMbLE
Deletion
LoxPsym
Inversion
Astaxanthin pathway
Translocation
YJJ001
YJJ168
YJJ432
b
200 kbp
7
6
5
4
3
2
1
0
-1
YJJ001
YJJ168
YJJ432
d
Astaxanthin yield (mg/g DCW)
3
2
1
0
YJJ001
YJJ168
YJJ432
Strains
c
synV
synX
Wild-type chromosomes
Telomere
YJJ001
YJJ168
YJJ432

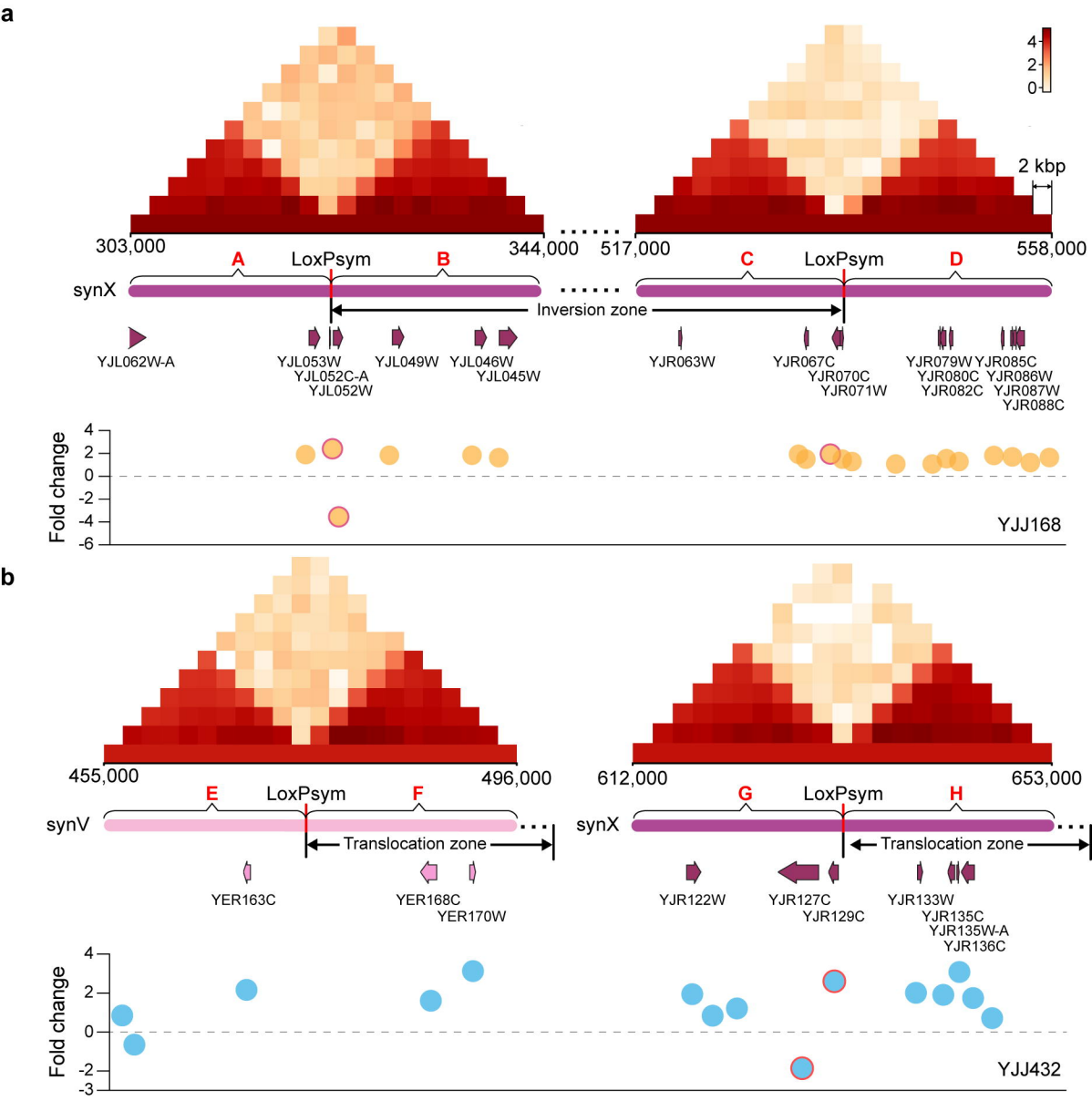
a
4
2
0
2 kbp
303,000
344,000
517,000
558,000
A
LoxPsym
B
C
LoxPsym
D
synX
Inversion zone
YJL062W-A
YJL053W
YJL052C-A
YJL052W
YJL049W
YJL046W
YJL045W
YJR063W
YJR067C
YJR070C
YJR071W
YJR079W
YJR080C
YJR082C
YJR085C
YJR086W
YJR087W
YJR088C
Fold change
4
2
0
-2
-4
-6
YJJ168
b
455,000
496,000
612,000
653,000
E
LoxPsym
F
G
LoxPsym
H
synV
Translocation zone
synX
Translocation zone
YER163C
YER168C
YER170W
YJR122W
YJR127C
YJR129C
YJR133W
YJR135C
YJR135W-A
YJR136C
Fold change
4
2
0
-2
-3
YJJ432

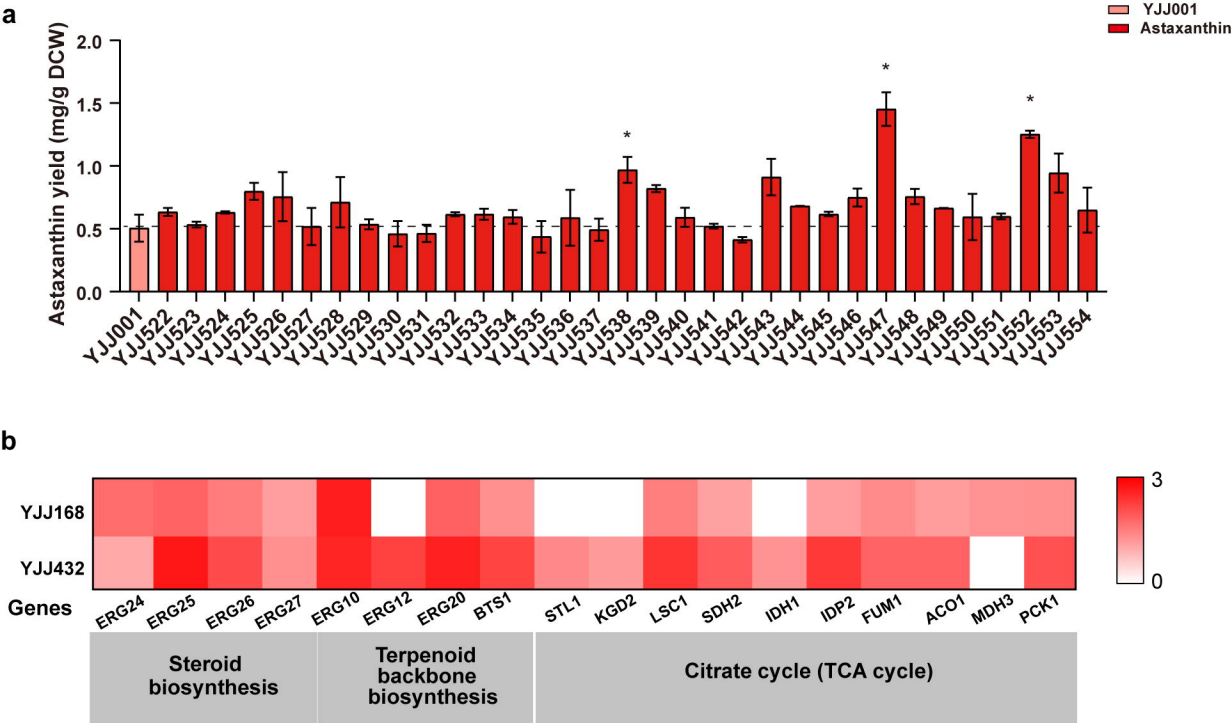
a
YJJ001
Astaxanthin
Astaxanthin yield (mg/g DCW)
2.0
1.5
1.0
0.5
0.0
*
*
*
YJJ001
YJJ522
YJJ523
YJJ524
YJJ525
YJJ526
YJJ527
YJJ528
YJJ529
YJJ530
YJJ531
YJJ532
YJJ533
YJJ534
YJJ535
YJJ536
YJJ537
YJJ538
YJJ539
YJJ540
YJJ541
YJJ542
YJJ543
YJJ544
YJJ545
YJJ546
YJJ547
YJJ548
YJJ549
YJJ550
YJJ551
YJJ552
YJJ553
YJJ554
b
YJJ168
YJJ432
Genes
ERG24
ERG25
ERG26
ERG27
ERG10
ERG12
ERG20
BTS1
STL1
KGD2
LSC1
SDH2
IDH1
IDP2
FUM1
ACO1
MDH3
PCK1
3
0
Steroid biosynthesis
Terpenoid backbone biosynthesis
Citrate cycle (TCA cycle)

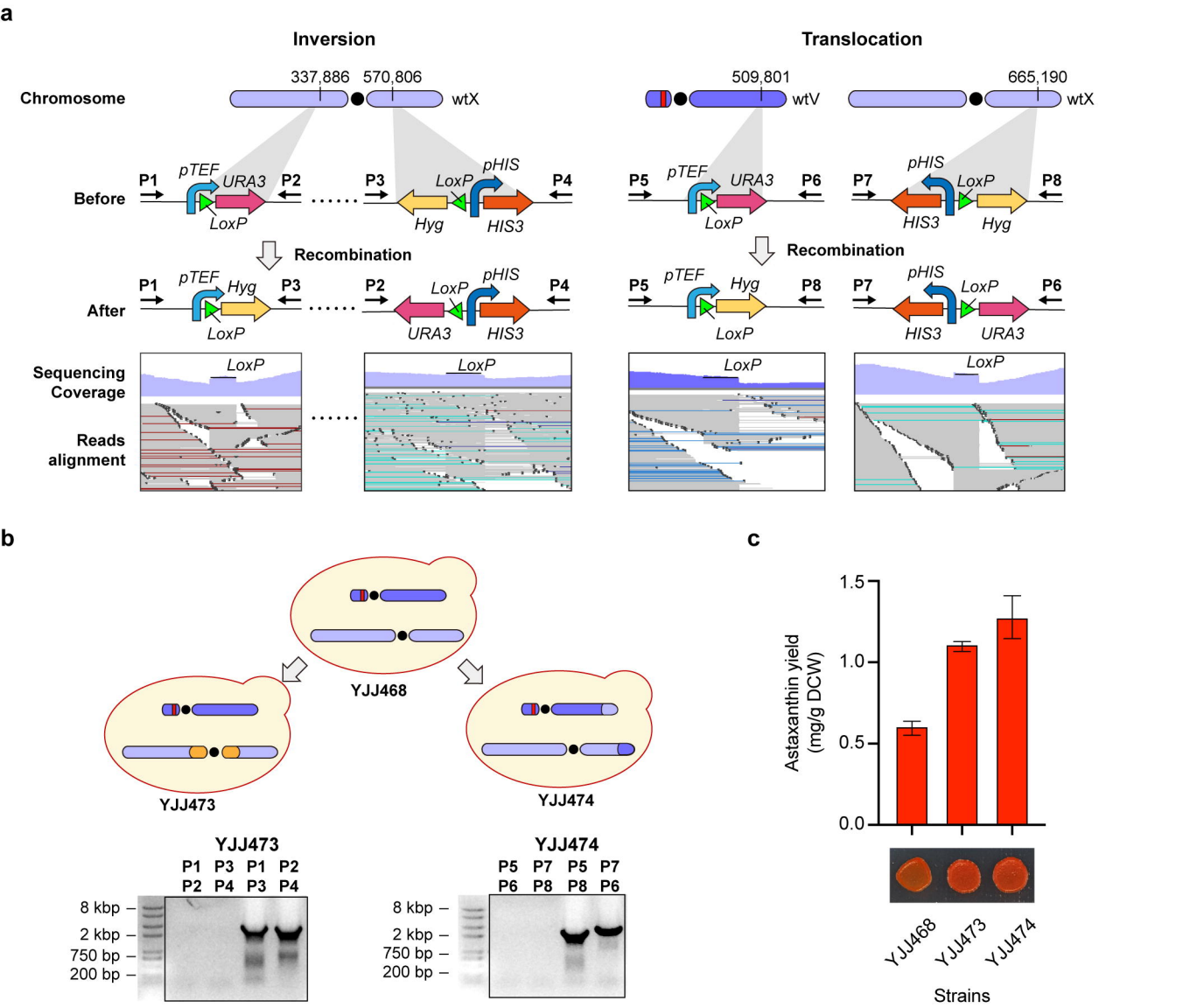
a
Inversion
Translocation
Chromosome
337,886
570,806
wtX
509,801
wtV
665,190
wtX
Before
P1
pTEF
URA3
P2
P3
LoxP
pHIS
P4
LoxP
Hyg
HIS3
P5
P6
P7
P8
Recombination
After
Hyg
Sequencing Coverage
Reads alignment
b
YJJ468
YJJ473
YJJ474
P1 P3 P1 P2
P2 P4 P3 P4
P5 P7 P5 P7
P6 P8 P8 P6
8 kbp
2 kbp
750 bp
200 bp
c
Astaxanthin yield (mg/g DCW)
1.5
1.0
0.5
0.0
YJJ468
YJJ473
YJJ474
Strains